Circulating Currents Suppression Based on Two Degrees of Freedom Control in DC Distribution Networks

Yanghong Xia, *Student Member, IEEE*, Yue Li, *Student Member, IEEE*, Yonggang Peng, *Member, IEEE*, Miao Yu, *Member, IEEE*, and Wei Wei

***Abstract*—In dc distribution networks, the parallel H-bridge dc/dc converters (HBDCs) are widely adopted to convert voltage levels with the higher power rating and reliability, in which the parallel HBDCs are naturally connected in input-parallel output-parallel (IPOP) form. However among IPOP HBDCs, there are complicated circulating currents that will influence the safe and steady operation of dc distribution networks. This paper focuses on the suppression of these circulating currents. First, the detailed mathematic models of circulating currents among IPOP HBDCs are derived. Through the model, it is found that various types of circulating currents exist in the system, including the circulating currents within the single HBDC and the circulating currents among the multiple HBDCs. Hence, the suppression of circulating currents among IPOP HBDCs is a multiobjective control problem. In this paper, it is proven that the conventional one degree of freedom control based on the bipolar modulation cannot eliminate all the circulating currents. Second, a novel two degrees of freedom control method is proposed to suppress all kinds of circulating currents based on the improved modulation way of HBDCs, which consists of two parts. The droop based control is used to suppress the circulating currents among the multiple HBDCs, whereas the common mode control is used to control the circulating currents within the single HBDC. All the theoretical analyses are verified by the real-time hardware-in-loop tests.**

***Index Terms*—Circulating currents, common mode control, dc distribution networks, input-parallel output-parallel (IPOP).**

I. Introduction

RECENTLY, more and more dc components are integrated into the power system no matter in the source side or the load side [1], [2]. First, in the source side, the penetration of renewable energy sources (RESs) is continuously increasing. Among the different RESs, solar photovoltaic generations, fuel cells, etc., are dc sources. Hence, another stage of conversion (dc to ac) is required if they are connected into ac distribution networks. Second, in the load side, the data centers, electric vehicles, etc., constitute a major part of the modern loads. All these loads are supplied by dc power. Therefore, the development of dc distribution networks can greatly improve the overall system efficiency [3]–[5].

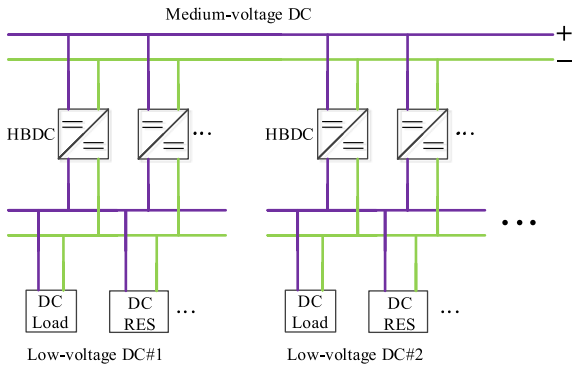

Fig. 1. Typical topology of a dc distribution network.

Fig. 1 presents a typical topology of the dc distribution network. The multiple low-voltage dc distribution networks are connected to the medium-voltage dc distribution network through parallel H-bridge dc/dc converters (HBDCs) to converter voltage levels. The low-voltage dc distribution networks provide dc power for the dc loads and integrate dc RESs. Because of the structure of the dc distribution network, these HBDCs are naturally connected in the input-parallel output-parallel (IPOP) form. The IPOP structures have following advantages [6]–[9]. On the one hand, due to the limitation of power rating of switching devices and the economic consideration, the single HBDC is hard to transform large power; the IPOP HBDCs can allow the use of low-power HBDC modules for high-power applications. On the other hand, the IPOP HBDCs have intrinsic redundancy and can provide ride-through capability when one of these HBDCs fails. Hence, the reliability of the dc distribution network is improved. However, due to the asymmetry of line resistances, the IPOP structure easily results in circulating currents, which increase the current stress on the switching devices, degrade system efficiency, or even cause system breakdown if not dealt appropriately.

The suppression methods of circulating currents among IPOP dc/dc converters are mainly classed into two categories. One

Manuscript received August 4, 2017; revised October 13, 2017; accepted November 20, 2017. Date of publication November 23, 2017; date of current version September 28, 2018. This work was supported in part by the National Key R&D Program of China (2017YFB0903300), in part by the National Natural Science Foundation of China under Grant 51377142, and in part by the Zhejiang Provincial Natural Science Foundation of China (LY16E070002). Recommended for publication by Associate Editor T.-F. Wu. *(Corresponding author: Yonggang Peng.)*

The authors are with the College of Electrical Engineering, Zhejiang University, Hangzhou 310027, China (e-mail: royxiayh@126.com; zju_liyue@zju.edu.cn; pengyg@zju.edu.cn; zjuyumiao@zju.edu.cn; wwei@zju.edu.cn).

Color versions of one or more of the figures in this paper are available online at http://ieeexplore.ieee.org.

Digital Object Identifier 10.1109/TPEL.2017.2777186

category is to change the topology of the converters based on the isolation solutions [8]–[11]. High-frequency isolation transformers can decouple the input side and output side, which can naturally eliminate the circulating currents within the single converter and only needs to suppress the circulating currents among the multiple converters. That is, it changes the multiobjective control problem into single-objective control problem. Hence, the suppression methods can be simplified. Shi *et al.* [8] split IPOP HBDCs into multiple IPOP dual-active half-bridge modules and utilizes a common-duty-ratio control scheme to realize the current sharing. Analogously, a modified topology with chain-connected rectifiers connecting multiple isolated half-bridge modules in the output terminal is proposed in [9], and the common-duty-ratio control scheme is used again to realize current sharing. However, the common-duty-ration control scheme basically treats the parallel converters as one converter, which makes the extension of converters inconveniently and has less redundancy. In [10], the changed IPOP HBDCs with isolation transformers connecting the output terminals are proposed, which are controlled by an interleaving control strategy. They can minimize and balance the capacitor ripple currents; hence, the circulating currents can be suppressed. Similarly, the extension is influenced because of the interleaving control strategy. In [11], the magnetic-coupling current-balancing cells based IPOP *LLC* resonant converter modules are designed, in which the input level consists of HBDCs, the intermediate level consists of isolation transformers, and the output level consists of rectifiers. The IPOP *LLC* resonant converter modules can work well under open-loop operating condition naturally. The aforementioned methods are based on the high-frequency isolation transformers, which are bulk and expensive. They may also suffer from both core and copper losses; hence, the efficiency and power density of the system are decreased.

Another category of suppression methods is to develop more advanced control methods without inserting the isolation transformers [12]–[16], which can enhance the efficiency and power density of the system. Compared to isolated dc/dc converters, the circulating currents among IPOP nonisolated dc/dc converters are more complicated with multiple types, including circulating currents both within the single converter and among the multiple converters. Through some simplifications, the model of circulating currents among IPOP nonisolated dc/dc converters is established in [13] and [14]. Furthermore, treating parallel converters as a whole, interleaved multiphase PWM schemes are proposed to reduce circulating currents. As mentioned above, the redundancy and extension are greatly influenced. These approaches are not suitable for modular application. When more converters are connected, the control system becomes very complicated to design. On the other hand, the proposed control methods cannot eliminate the circulating currents within the single converter. The topology of single-phase ac/dc converter is the same as the HBDC. Through graphics, the generation mechanism of circulating currents among IPOP single-phase ac/dc converters is qualitatively analyzed in [15] and [16]. Then, a simplified PWM with switching constraint method is proposed to suppress the circulating currents. But the analysis about the generation mechanism of circulating currents among IPOP single-phase ac/dc converters lacks of detailed quantitative analysis. Furthermore, the proposed control methods can only work well when the line resistances are symmetric.

From the above narration, it can be concluded that the suppression of circulating currents among IPOP nonisolated HBDCs in dc distribution networks is not well solved. Focusing on this problem, this paper proposes two degrees of control method to suppress the circulating currents among the IPOP HBDCs. First, the detailed mathematic model of the circulating currents is derived. Through the model, the complicated characteristics and the corresponding influence factors of the circulating currents are analyzed. It is found that there are various types of circulating currents including circulating currents within the single HBDC and circulating currents among the multiple HBDCs. Hence, the suppression of circulating currents among IPOP HBDCs is a multiobjective control problem. The asymmetry of both input and output line resistances can result in great circulating currents. The circulating currents within the single HBDC cause port degradation of the converter, that is, the positive and negative currents of one converter are unequal. The port degradation will make some port-based control methods ineffective and influence the relay protection. Furthermore, it will increase the orders of the system model and make the system model more complicated. At the same time, from the point of degrees of freedom, we have proven that the conventional bipolar modulation based control methods with only one degree of freedom cannot eliminate all the circulating currents. Second, based on the analysis of circulating currents, a decentralized two degrees of freedom control method is proposed to suppress all kinds of circulating currents based on the improved modulation way of HBDCs. The improved modulation way has two degrees of freedom. That is, unlike the bipolar modulation, the two bridge legs of one HBDC can be controlled independently. Based on this, the proposed control method contains two parts. The droop based control namely the second degree of freedom control is used to suppress the circulating currents among the multiple HBDCs, whereas the common mode control namely the first degree of freedom control is used to control the circulating currents within the single HBDC. The proposed control method is fully decentralized, the control for one HBDC module does not need information of other HBDC modules. Thus, it is suitable for modular application very well. All the theoretical analyses are verified by the real-time hardware-in-loop (HIL) tests mainly composed of the RTLAB and STM32F407 MCUs.

The remainder of this paper is organized as follows. In Section II, the modeling and analysis of circulating currents among IPOP HBDCs are conducted. The proposed decentralized two degrees of freedom control method is introduced in Section III. In Section IV, the validity of the analyses is demonstrated through HIL tests. At last, the conclusions are drawn in Section V.

II. Modeling and Analysis of Circulating Currents Among IPOP HBDCs

A. Modeling

For convenience, we illustrate related problems through two IPOP HBDCs, but the methods and conclusions can be extended to $N\,(N > 2)$ IPOP HBDCs with more complicated expressions.

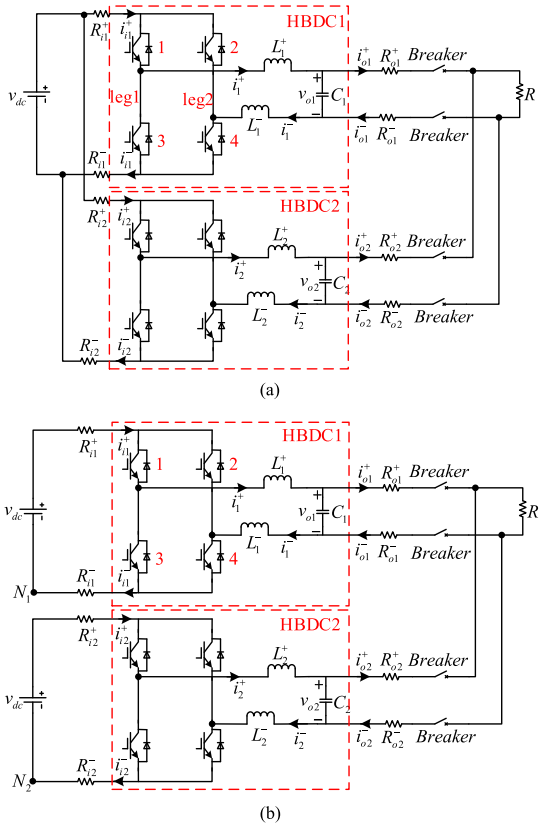

Fig. 2. Structures of two HBDCs connected in (a) IPOP form and (b) ISOP form.

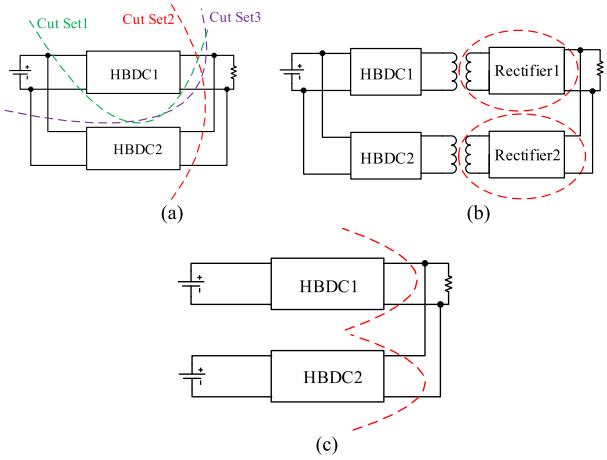

Fig. 3. Comparison among various structures. (a) Currents coupling of IPOP HBDCs. (b) Currents decoupling of IPOP isolated HBDCs. (c) Currents decoupling of ISOP HBDCs.

The structure of two IPOP HBDCs is shown in Fig. 2 (a), where the components of dc distribution networks are simplified and only the main characteristics are taken into consideration. The two HBDCs operate in coordination to convert the medium voltage $v_{\rm dc}$ to low voltage and to provide power for the load R. The outputs of HBDCs are filtered by LC filters whose inductances are L_1^+, L_1^- and L_2^+, L_2^-, capacitances are C_1 and C_2, respectively. The positive input line resistances are R_{i1}^+ and R_{i2}^+, respectively, whereas the negative input line resistances are R_{i1}^- and R_{i2}^-, respectively. The positive output line resistances

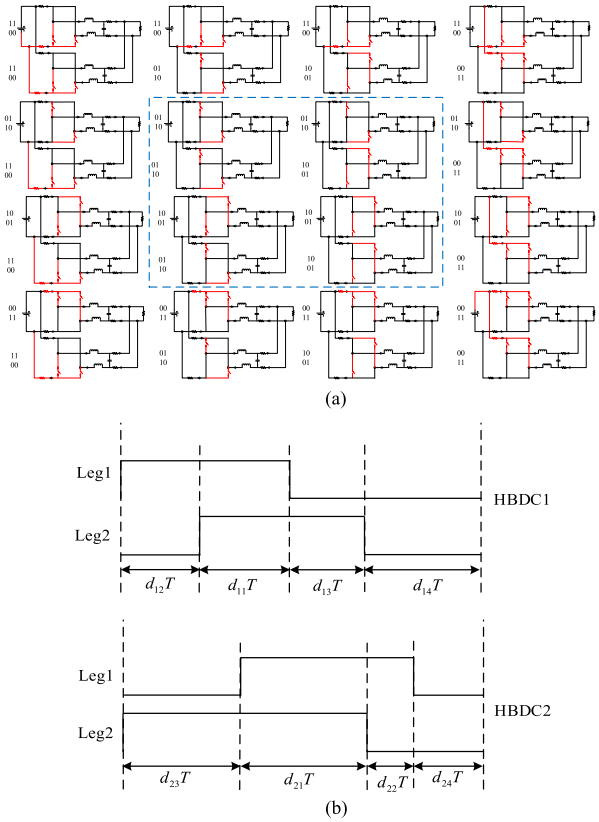

Fig. 4. Operating states of two IPOP HBDCs. (a) 16 different operating states. (b) Sketches of duty ratios.

are R_{o1}^+ and R_{o2}^+, respectively, whereas the negative output line resistances are R_{o1}^- and R_{o2}^-, respectively. The breakers of positive and negative poles are used to protect the HBDCs from faults like overcurrent etc. Fig. 2 (b) shows the structure of two input-separated output-parallel (ISOP) HBDCs, the meanings of corresponding notations are the same as those in the Fig. 2 (a). The ISOP structures are widely applied in dc microgrids to make different RESs integrate into the power system. Comparing Fig. 2 (a) with (b), the essential difference between IPOP HBDCs in dc distribution networks and ISOP HBDCs in dc microgrids is that the potentials of points N_1 and N_2 are clamped in IPOP HBDCs. This difference will result in the model of IPOP HBDCs with more constraints, then, makes the model more complicated than the model of ISOP HBDCs.

The IPOP HBDCs are nonisolated topology, which can enhance the efficiency and power density of the converters, but the currents of IPOP HBDCs are coupled together. As Fig. 3 (a) shows, according to Kirchhoff's laws, the sum of output currents and input currents of cut set1 is zero, that is, $i_{o1}^+ - i_{o1}^- = i_{i1}^+ - i_{i1}^-$, which cannot represent $i_{o1}^+ - i_{o1}^- = 0$. Through the analyses of cut set2 and cut set3, the similar conclusions can be obtained, that is, the positive currents are not always equal to the negative currents, which is called port degradation in this paper. Because of the port degradation, there will be multiple types of circulating currents including the circulating currents within the single HBDC and circulating currents among the multiple HBDCs. Then, the suppression of circulating currents among IPOP HBDCs is more challenging.

But for the IPOP isolated HBDCs, the positive currents are always equal to the negative currents, which can be obviously verified through the cut sets in Fig. 3 (b). Since there are no circulating currents within the single HBDC, the suppression becomes easier than that of IPOP HBDCs with only consideration of circulating currents among the multiple HBDCs. But due to the existence of high-frequency isolation transformers, the volume and losses (core and copper losses) of converters will increase; hence, the efficiency and power density of the system are decreased. Similarly, for the ISOP HBDCs, the positive currents are always equal to the negative currents, which can be obviously verified through the cut sets in Fig. 3 (c). Hence, in the application scenarios of this kind of ISOP structure such as dc microgrids to make different RESs integrate into the power system, the droop control can suppress the circulating currents well because only the circulating currents among the multiple HBDCs exist [17]–[19]. However, for the IPOP HBDCs, the droop control cannot eliminate all kinds of circulating currents.

As Fig. 4 shows, there are 16 operating stages of two IPOP HBDCs according to the on–off states of HBDC1 and HBDC2. Based on Fig. 2 (a) and Fig. 4, the average model of switch cycle can be derived as

$$\begin{cases} L_1^+\frac{di_1^+}{dt}+L_1^-\frac{di_1^-}{dt}+\left(d_{12}R_{i1}^+ + d_{13}R_{i1}^-\right)i_1^+ \\ \quad +\left(d_{13}R_{i1}^+ + d_{12}R_{i1}^-\right)i_1^- + v_{o1} = (d_{12}-d_{13})\ v_{\rm dc} \\ \left(i_1^+ - C_1\frac{dv_{o1}}{dt}\right)R_{o1}^+ + \left(i_1^- - C_1\frac{dv_{o1}}{dt}\right)R_{o1}^- \\ \quad +\left(i_1^+ - C_1\frac{dv_{o1}}{dt} + i_2^+ - C_2\frac{dv_{o2}}{dt}\right)R = v_{o1} \\ L_2^+\frac{di_2^+}{dt}+L_2^-\frac{di_2^-}{dt}+\left(d_{22}R_{i2}^+ + d_{23}R_{i2}^-\right)i_2^+ \\ \quad +\left(d_{23}R_{i2}^+ + d_{22}R_{i2}^-\right)i_2^- + v_{o2} = (d_{22}-d_{23})\ v_{\rm dc} \\ \left(i_2^+ - C_2\frac{dv_{o2}}{dt}\right)R_{o2}^+ + \left(i_2^- - C_2\frac{dv_{o2}}{dt}\right)R_{o2}^- \\ \quad +\left(i_1^+ - C_1\frac{dv_{o1}}{dt} + i_2^+ - C_2\frac{dv_{o2}}{dt}\right)R = v_{o2} \\ i_1^+ + i_2^+ = i_1^- + i_2^- \\ L_1^+\frac{di_1^+}{dt}+\left(i_1^+ - C_1\frac{dv_{o1}}{dt}\right)R_{o1}^+ + \left(d_{11}R_{i1}^+ + d_{14}R_{i1}^-\right) \\ \quad \times\left(i_1^+ - i_1^-\right)+\left(d_{12}R_{i1}^+ + d_{13}R_{i1}^-\right)i_1^+ - (d_{12}+d_{11})\,v_{\rm dc} \\ = L_2^+\frac{di_2^+}{dt}+\left(i_2^+ - C_2\frac{dv_{o2}}{dt}\right)R_{o2}^+ + \left(d_{21}R_{i2}^+ + d_{24}R_{i2}^-\right) \\ \quad \times\left(i_2^+ - i_2^-\right)+\left(d_{22}R_{i2}^+ + d_{23}R_{i2}^-\right)i_2^+ - (d_{22}+d_{21})\,v_{\rm dc} \end{cases} \tag{1}$$

where the duty ratios are shown in Fig. 4 (b). When the duty ratio of leg1 is "1," the upper tube (tube1) is on and lower tube (tube3) is off. When the duty ratio of leg1 is "0," the upper tube (tube1) is off and lower tube (tube3) is on. The meaning of the duty ratio of leg2 is similar. Hence, there are four combinations of the on–off states between leg1 and leg2. The duty ratios of different states are represented by $d_{k,1}$, $d_{k,2}$, $d_{k,3}$, and $d_{k,4}$ as shown in Fig. 4 (b), where $k = 1, 2$ represents the different HBDCs.

Equation (1) is a typical differential algebraic equation; hence, we need to choose independent state variables to reduce the orders of the system. Choose i_1^+, i_1^-, v_{o1}, i_2^+, v_{o2} as the state variables, the standard state space model of IPOP HBDCs can be obtained as follows:

$$\boldsymbol{A}\,\dot{\boldsymbol{X}} = \boldsymbol{B}\boldsymbol{X} + \boldsymbol{U} \tag{2}$$

where $\boldsymbol{X} = [i_1^+\ i_1^-\ v_{o1}\ i_2^+\ v_{o2}]^{\rm T}$, unnumbered Eqn. shown at the bottom of this page.

For the two ISOP HBDCs, consider that $i_k^+ = i_k^-$ $(k = 1, 2)$ and then let $i_k^+ = i_k^- = i_k$ $(k = 1, 2)$, based on Fig. 2 (b) and Fig. 4, the average model of switch cycle can be derived as

$$\begin{cases} \left(L_1^+ + L_1^-\right)\frac{di_1}{dt} + \left(d_{12}+d_{13}\right)\left(R_{i1}^+ + R_{i1}^-\right)i_1 + v_{o1} \\ \quad = (d_{12}-d_{13})\ v_{\rm dc} \\ \left(i_1 - C_1\frac{dv_{o1}}{dt}\right)\left(R_{o1}^+ + R_{o1}^-\right) + \left(i_1 - C_1\frac{dv_{o1}}{dt} + i_2 - C_2\frac{dv_{o2}}{dt}\right) \\ \quad \times R = v_{o1} \\ \left(L_2^+ + L_2^-\right)\frac{di_2}{dt} + \left(d_{22}+d_{23}\right)\left(R_{i2}^+ + R_{i2}^-\right)i_2 + v_{o2} \\ \quad = (d_{22}-d_{23})\ v_{\rm dc} \\ \left(i_2 - C_2\frac{dv_{o2}}{dt}\right)\left(R_{o2}^+ + R_{o2}^-\right) + \left(i_1 - C_1\frac{dv_{o1}}{dt} + i_2 - C_2\frac{dv_{o2}}{dt}\right) \\ \quad \times R = v_{o2} \end{cases} \tag{3}$$

where the duty ratios are shown in Fig. 4 (b).

According to (3), the standard state-space model of ISOP HBDCs can be obtained as follows, (4) shown at the bottom of the next page.

Comparing (2) and (4), it can be concluded that the model of two IPOP HBDCs is more complicated than the model of two ISOP HBDCs. The orders of IPOP HBDCs (fifth-order model) are increased than the orders of ISOP HBDCs

$$\boldsymbol{A} = \begin{bmatrix} L_1^+ & L_1^- & 0 & 0 & 0 \\ 0 & 0 & \left(R_{o1}^+ + R_{o1}^- + R\right)C_1 & 0 & RC_2 \\ L_2^- & -L_2^- & 0 & L_2^+ + L_2^- & 0 \\ 0 & 0 & RC_1 & 0 & \left(R_{o2}^+ + R_{o2}^- + R\right)C_2 \\ L_1^+ & 0 & -R_{o1}^+C_1 & -L_2^+ & R_{o2}^+C_2 \end{bmatrix},\quad \boldsymbol{U} = \begin{bmatrix} (d_{12}-d_{13})\,v_{\rm dc} \\ 0 \\ (d_{22}-d_{23})\,v_{\rm dc} \\ 0 \\ (d_{11}+d_{12}-d_{21}-d_{22})\,v_{\rm dc} \end{bmatrix}$$

$$\boldsymbol{B} = \begin{bmatrix} -\left(d_{12}R_{i1}^+ + d_{13}R_{i1}^-\right) & -\left(d_{13}R_{i1}^+ + d_{12}R_{i1}^-\right) & -1 & 0 & 0 \\ R_{o1}^+ + R & R_{o1}^- & -1 & R & 0 \\ -\left(d_{23}R_{i2}^+ + d_{22}R_{i2}^-\right) & d_{23}R_{i2}^+ + d_{22}R_{i2}^- & 0 & -\left(d_{22}+d_{23}\right)\left(R_{i2}^+ + R_{i2}^-\right) & -1 \\ R_{o2}^- + R & -R_{o2}^- & 0 & R_{o2}^+ + R_{o2}^- + R & -1 \\ -R_{o1}^+ - (d_{11}+d_{12})\left(R_{i1}^+ - R_{i1}^-\right) & d_{11}R_{i1}^+ + d_{14}R_{i1}^- + d_{21}R_{i2}^+ + d_{24}R_{i2}^- & 0 & R_{o2}^+ + d_{22}R_{i2}^+ + d_{23}R_{i2}^- & 0 \\ -R_{i1}^- - d_{21}R_{i2}^+ - d_{24}R_{i2}^- & & & & \end{bmatrix}$$

TABLE I
SYSTEM PARAMETERS OF IPOP HBDCS

Parameters	Rated Value
v_{dc}	1000 V
R	2 Ω
$d_{11}, d_{12},\ d_{13}, d_{14}$	0.0, 0.8, 0.2, 0.0
$d_{21}, d_{22},\ d_{23}, d_{24}$	0.0, 0.8, 0.2, 0.0
$L_1^+, L_1^-, L_2^+, L_2^-$	0.5 mH, 0.5 mH, 0.5 mH, 0.5 mH
C_1, C_2	8 mF, 8 mF
$R_{i1}^-,\ R_{i1}^+, R_{i2}^-,\ R_{i2}^+$	0.01 Ω, 0.01 Ω, 0.01 Ω, 0.01 Ω
$R_{o1}^-,\ R_{o1}^+, R_{o2}^-,\ R_{o2}^+$	0.01 Ω, 0.01 Ω, 0.01 Ω, 0.01 Ω

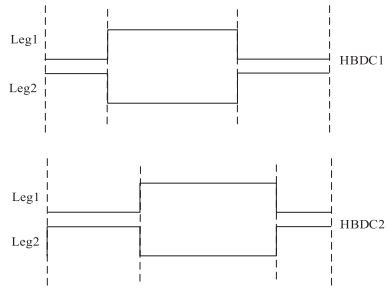

Fig. 5. Sketches of duty ratios based on bipolar modulation.

(fourth-order model). For the general case, the orders of *N* IPOP HBDCs are 3*N*−1, whereas the orders of *N* ISOP HBDCs are 2*N*. Furthermore, it can be easily found that for ISOP HBDCs, the filters and line resistances of positive poles and negative poles can be combined together, that is, their effects are equal to inductances $L_k^+ + L_k^-$ and the resistances $R_{i,k}^+ + R_{i,k}^-$ or $R_{o,k}^+ + R_{o,k}^-(k\ = 1, 2)$. However, for IPOP HBDCs, the filters and line resistances of positive poles and negative poles must be considered separately.

B. Analysis

To further reveal the aspects of IPOP HBDCs, this part mainly studies the dynamic and steady characteristics of IPOP HBDCs under the open-loop control according to the model established in part A.

From (2), the poles of IPOP HBDCs can be solved through solving the eigenvalues of matrix $\boldsymbol{A}^{-1}\boldsymbol{B}$. The poles of IPOP HBDCs can directly reflect the dynamic characteristics. Similarly, the steady output values of IPOP HBDCs can be solved through calculating $-\boldsymbol{B}^{-1}\boldsymbol{U}$ in (2). In steady state, $i_{o,k}^+ = i_k^+$ and $i_{o,k}^- = i_k^-\ (k\ = 1, 2)$. Then, the circulating currents can be obtained, which can reflect the steady characteristics. The rated system parameters are shown in Table I, where the modulation way is the conventional bipolar modulation, that is, the switching signals of leg1 and leg2 are complementary ($d_{k,2} + d_{k,3} = 1$, $k\ = 1, 2$)as shown in Fig. 5. When the conventional bipolar modulation is adopted, the operating states of IPOP HBDCs are decreased into four states as identified through blue dashed box in Fig. 4 (a).

Fig. 6 (a) shows the dominant poles of IPOP HBDCs with the changes of filter inductances of HBDC1, where $L_1^+ + L_1^- =$ 1 mH but their ratio L_1^-/L_1^+ changes. The figure reflects the dynamic characteristics of IPOP HBDCs. From the figure, it can be seen that the asymmetry of positive and negative filter inductances will influence the dynamics of the IPOP HBDCs even though their sum remains unchanged. But for the ISOP HBDCs, the dynamics will keep unchanged as long as the sum of positive and negative filter inductances remains unchanged, which can be easily proven through (4). This phenomenon indicates that the IPOP HBDCs have unique characteristics and are greatly different from the ISOP HBDCs.

Fig. 6 (b) shows the circulating currents among IPOP HBDCs with the changes of input line resistances of HBDC1, where $R_{i1}^+ + R_{i1}^- = 0.02\ \Omega$ but their ratio R_{i1}^-/R_{i1}^+ changes. The figure reflects the steady characteristics of IPOP HBDCs. As the figure shows, the asymmetry of the positive and negative input line resistances of HBDC1 can cause great circulating currents even though their sum keeps the same as that of HBDC2. Furthermore, it can be found that there are various types of circulating currents including circulating currents within the single HBDC, e.g., $i_{o1}^+ - i_{o1}^-$ and $i_{o2}^+ - i_{o2}^-$, circulating currents among the multiple HBDCs, e.g., $i_{o1}^+ - i_{o2}^+$ and $i_{o1}^- - i_{o2}^-$. But for the ISOP HBDCs, there will be no circulating currents as long as the sums of positive and negative input line resistances of different HBDCs keep the same, which can also be easily proven through (4). This phenomenon indicates that the circulating currents among IPOP HBDCs are more complicated than the circulating currents among ISOP HBDCs. Hence, the corresponding suppression method is more challenging.

$$\begin{bmatrix} L_1^+ + L_1^- & 0 & 0 & 0 \\ 0 & \left(R_{o1}^+ + R_{o1}^- + R\right) C_1 & 0 & RC_2 \\ 0 & 0 & L_2^+ + L_2^- & 0 \\ 0 & RC_1 & 0 & \left(R_{o2}^+ + R_{o2}^- + R\right) C_2 \end{bmatrix} \begin{bmatrix} \frac{di_1}{dt} \\ \frac{dv_{o1}}{dt} \\ \frac{di_2}{dt} \\ \frac{dv_{o2}}{dt} \end{bmatrix}$$
$$= \begin{bmatrix} -\left(d_{12} + d_{13}\right)(R_{i1}^+ + R_{i1}^-) & -1 & 0 & 0 \\ R_{o1}^+ + R_{o1}^- + R & -1 & R & 0 \\ 0 & 0 & -\left(d_{22} + d_{23}\right)(R_{i2}^+ + R_{i2}^-) & -1 \\ R & 0 & R_{o2}^+ + R_{o2}^- + R & -1 \end{bmatrix} \begin{bmatrix} i_1 \\ v_{o1} \\ i_2 \\ v_{o2} \end{bmatrix} + \begin{bmatrix} \left(d_{12} - d_{13}\right) v_{\mathrm{dc}} \\ 0 \\ \left(d_{22} - d_{23}\right) v_{\mathrm{dc}} \\ 0 \end{bmatrix} \tag{4}$$

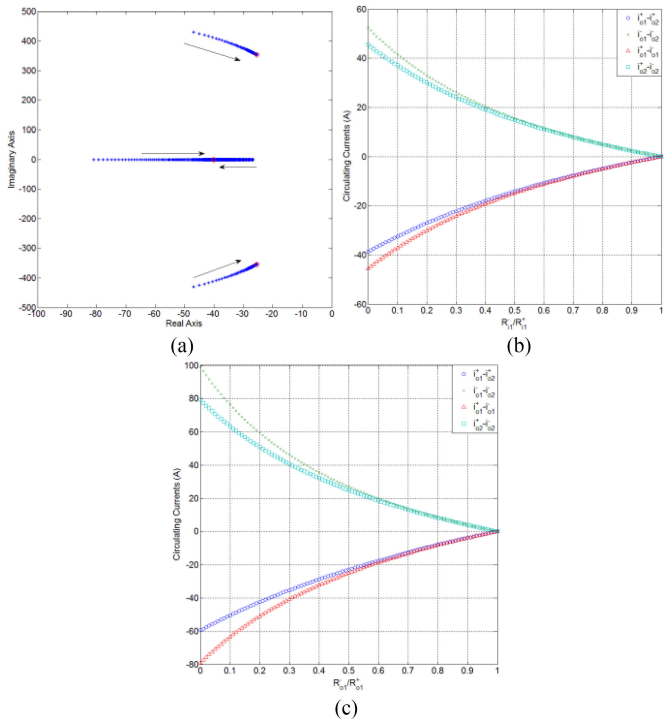

Fig. 6. Dynamic and steady characteristics of IPOP HBDCs. (a) Dominant poles when $L_1^+ + L_1^- = 1$ mH but L_1^-/L_1^+ changes from 0 to 1. (b) Circulating currents when $R_{i1}^+ + R_{i1}^- = 0.02\ \Omega$ but R_{i1}^-/R_{i1}^+ changes from 0 to 1. (c) Circulating currents when $R_{o1}^+ + R_{o1}^- = 0.02\ \Omega$ but R_{o1}^-/R_{o1}^+ changes from 0 to 1.

The influences of output line resistances are studied in similar ways, which are shown in Fig. 6 (c), where $R_{o1}^+ + R_{o1}^- = 0.02\ \Omega$ but their ratio R_{o1}^-/R_{o1}^+ changes. Compared to Fig. 6 (b), it can be concluded that the asymmetry of the positive and negative output line resistances of HBDC1 has greater influences on circulating currents than input line resistances.

On the other hand, due to the existence of circulating currents within the single HBDC, it can be seen that the port degradation is obvious, that is, $i_{o1}^+ - i_{o1}^- \neq 0$ or $i_{o2}^+ - i_{o2}^- \neq 0$, which means that the fundamental property of a port that the positive and negative currents must be equal cannot be ensured. Hence, the output terminal or input terminal of a single HBDC module in IPOP HBDCs cannot be viewed as a port anymore. The port degradation can be viewed as the generalization of zero-sequence circulating currents in three-phase ac/dc converters [20]–[23]. Some port-based control methods will be ineffective because of the port degradation [24]–[27]. Taking the impedance analysis as an example. Because the output currents of positive and negative poles are different, the concept of "impedance" is hard to define in dc system. Therefore, the impedance analysis will be challenged and needs to extend. Furthermore, the port degradation will influence relay protection. Usually, the breakers of the positive and the negative poles are set the same protection values. If the port degradation is not considered, the breakers will act frequently because of the great differences between the positive and negative currents.

The conventional droop control applied to ISOP HBDCs cannot suppress the circulating currents among IPOP HBDCs effectively [17]–[19]. Assuming the droop control using the positive currents i_{o1}^+ and i_{o2}^+ as feedback signals, then the equivalent control effects of droop control can be thought that two same resistances namely the droop coefficients ($\gg$positive output line resistances) are added to the positive poles to make the equivalent positive output line resistances equal. However, there is no guarantee that the negative output line resistances are the same as the equivalent positive output line resistances. Then, the circulating currents can still exist as shown in Fig. 6 (c). That is, the conventional droop control cannot suppress the circulating currents among IPOP HBDCs effectively.

Now, we prove that the conventional bipolar modulation cannot suppress all kinds of circulating currents among IPOP HBDCs. In steady state, assume existing duty ratios that can eliminate circulating currents. Because of the bipolar modulation, the following equations can be derived

$$\begin{cases} d_{13} = 1 - d_{12} \\ d_{23} = 1 - d_{22} \\ d_{11} = d_{14} = d_{21} = d_{24} = 0 \end{cases}. \tag{5}$$

Then, let $i_{o1}^+ = i_{o1}^- = i_{o2}^+ = i_{o2}^- = I$ and consider that $i_{o,k}^+ = i_k^+$, $i_{o,k}^- = i_k^-$ $(k = 1, 2)$ in steady state. The following steady-state equations can be derived according to (1) and (5)

$$\begin{cases} \left(R_{i1}^+ + R_{i1}^- + R_{o1}^+ + R_{o1}^- + 2R\right) I = (2d_{12} - 1)\ v_{\rm dc} \\ \left(R_{i2}^+ + R_{i2}^- + R_{o2}^+ + R_{o2}^- + 2R\right) I = (2d_{22} - 1)\ v_{\rm dc} \\ \left[d_{12}\left(R_{i1}^+ - R_{i1}^-\right) + R_{i1}^- + R_{o1}^+\right] I - d_{12} v_{\rm dc} \\ \quad = \left[d_{22}\left(R_{i2}^+ - R_{i2}^-\right) + R_{i2}^- + R_{o2}^+\right] I - d_{22} v_{\rm dc} \end{cases}. \tag{6}$$

For (6), there are only two independent unknown variables but three constraint equations. Hence, for arbitrary line resistances and I, there is no duty ratios that can meet the equations. That is, for the general case, the conventional bipolar modulation cannot completely eliminate all types of circulating currents among IPOP HBDCs.

In fact, through (5) and Fig. 5, it can be found that the bipolar modulation is only with one degree of freedom. But the circulating currents among IPOP HBDCs contain two independent types, hence, the bipolar modulation cannot eliminate these two kinds of circulating currents at the same time.

III. Description of the Proposed Control Method

In Section II, the detailed mathematic model and characteristics of circulating currents among IPOP HBDCs are introduced. And it is proven that the conventional bipolar modulation based control methods with only one degree of freedom cannot eliminate all kinds of circulating currents among IPOP HBDCs. This section mainly introduces the proposed control method that can suppress the circulating currents effectively.

As mentioned above, the conventional bipolar modulation cannot eliminate circulating currents among IPOP HBDCs completely. In this paper, a novel modulation way based on common mode and differential mode is proposed to overcome the disadvantages of bipolar modulation. As shown in Fig. 7 (a), the two

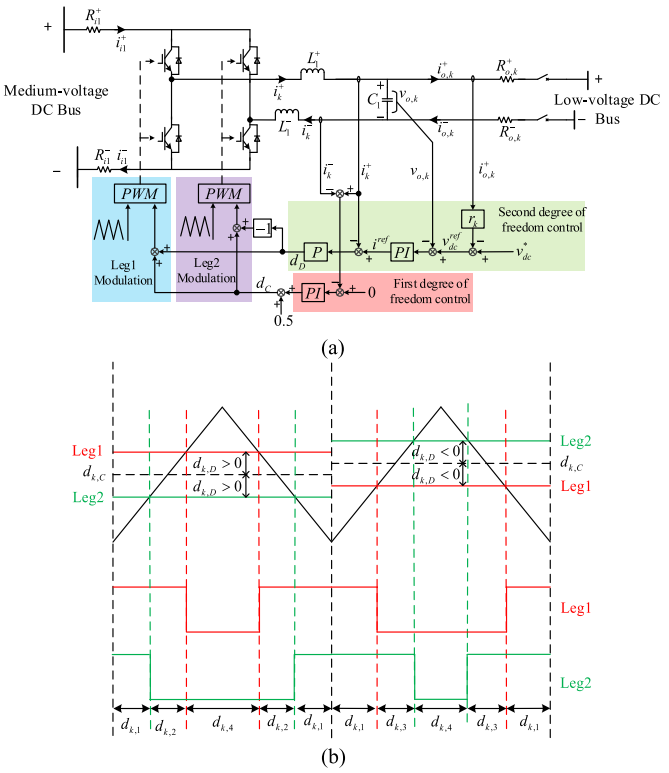

Fig. 7. Proposed two degrees of freedom control method. (a) Control block of the proposed control method for kth HBDC. (b) Proposed modulation way.

legs of one HBDC are modulated, respectively. The duty ratios of two legs can be expressed as follows

$$\begin{cases} \text{Leg1} : d_{k,C} + d_{k,D} \\ \text{Leg2} : d_{k,C} - d_{k,D} \end{cases} \tag{7}$$

where $k = 1, 2$ represents different HBDCs, $d_{k,C}$ represents common mode components, and $d_{k,D}$ represents differential mode components.

According to (7) and Fig. 7 (b), the corresponding duty ratios of Fig. 4 can be calculated as

$$\begin{cases} d_{k,1} = d_{k,C} - |d_{k,D}| \\ d_{k,4} = 1 - d_{k,C} - |d_{k,D}| \\ d_{k,2} = 2h\left(d_{k,D}\right)|d_{k,D}| \\ d_{k,3} = 2\left(1 - h\left(d_{k,D}\right)\right)|d_{k,D}| \end{cases} \tag{8}$$

where $h\left(d_{k,D}\right) = 1$ if $d_{k,D} \geq 0$, $h\left(d_{k,D}\right) = 0$ if $d_{k,D} < 0$. From (7) and (8), it can be concluded that the proposed modulation way has two degrees of freedom namely $d_{k,C}$ and $d_{k,D}$, which can make the most of two legs.

Now, we prove that the proposed the modulation way can realize the suppression of circulating currents among IPOP HBDCs. Similarly, in steady state, assume existing duty ratios that can eliminate circulating currents. Then, let $i_{o1}^{+} = i_{o1}^{-} = i_{o2}^{+} = i_{o2}^{-} = I$ and consider that $i_{o,k}^{+} = i_{k}^{+}$, $i_{o,k}^{-} = i_{k}^{-}$ $(k = 1, 2)$ in steady state. The following steady-state equations can be derived according to (1) and (8)

$$\begin{cases} \left[2\left|d_{1D}\right|\left(R_{i1}^{+} + R_{i1}^{-}\right) + R_{o1}^{+} + R_{o1}^{-} + 2R\right] I \\ \quad = \left(4h\left(d_{1D}\right)\left|d_{1D}\right| - 2\left|d_{1D}\right|\right) v_{\mathrm{dc}} \\ \left[2\left|d_{2D}\right|\left(R_{i2}^{+} + R_{i2}^{-}\right) + R_{o2}^{+} + R_{o2}^{-} + 2R\right] I \\ \quad = \left(4h\left(d_{2D}\right)\left|d_{2D}\right| - 2\left|d_{2D}\right|\right) v_{\mathrm{dc}} \\ \left[2h\left(d_{1D}\right)\left|d_{1D}\right|\left(R_{i1}^{+} - R_{i1}^{-}\right) + 2\left|d_{1D}\right| R_{i1}^{-} + R_{o1}^{+}\right] I \\ \quad - \left(d_{1C} - \left|d_{1D}\right| + 2h\left(d_{1D}\right)\left|d_{1D}\right|\right) v_{\mathrm{dc}} \\ = \left[2h\left(d_{2D}\right)\left|d_{2D}\right|\left(R_{i2}^{+} - R_{i2}^{-}\right) + 2\left|d_{2D}\right| R_{i2}^{-} + R_{o2}^{+}\right] I \\ \quad - \left(d_{2C} - \left|d_{2D}\right| + 2h\left(d_{2D}\right)\left|d_{2D}\right|\right) v_{\mathrm{dc}} \end{cases} \tag{9}$$

From (9), it can be found that there are four independent unknown variables but only three constraint equations. Hence, the proposed modulation way can eliminate all kinds of circulating currents among IPOP HBDCs.

Concretely, the two degrees of freedom $d_{k,C}$ and $d_{k,D}$ are used to suppress different kinds of circulating currents. As shown in Fig. 7 (a), the first degree of freedom $d_{k,C}$, namely the common mode components, is used to control the circulating currents within the single HBDC. The difference between the positive current and the negative current $i_{k}^{-} - i_{k}^{+}$ is sent to a proportional-integral (PI) controller, which regulates $d_{k,C}$ to make $i_{k}^{-} - i_{k}^{+}$ equal zero. Then, the circulating currents within the single HBDC can be suppressed. The control law can be expressed as

$$d_{k,C} = 0.5 + \left(k_{\mathrm{CP}} + \frac{k_{\mathrm{CI}}}{s}\right)\left(i_{k}^{-} - i_{k}^{+}\right) \tag{10}$$

where k_{CP} is the proportional coefficient, k_{CI} is the integral coefficient.

For the circulating currents among the multiple HBDCs, the droop-based control strategy is adopted as shown in Fig. 7 (a), which mainly regulates the second degree of freedom $d_{k,D}$ namely the differential mode components. The second degree of freedom control consists of two parts. The outer loop is the typical droop control, which is used to realize current sharing among HBDCs. That is, the circulating currents among the multiple HBDCs can be suppressed effectively. The control law can be expressed as

$$v_{\mathrm{dc},k}^{\mathrm{ref}} = v_{\mathrm{dc}}^{*} - r_k i_{o,k}^{+} \tag{11}$$

where r_k is the droop coefficient, v_{dc}^{*} is the rated low voltage, $v_{\mathrm{dc},k}^{\mathrm{ref}}$ is the reference output voltage for the inner loop.

The inner loop of the second degree of freedom control is composed of dual-loop control. The current loop controls the current i_{k}^{+} with a proportional controller k_{iP} to increase the damping of the system and to make the system more stable. The voltage loop controls the output voltage $v_{o,k}$ with a PI controller $k_{vP} + \frac{k_{vI}}{s}$ to realize the accurate tracking.

Through the two degrees of freedom control, both the circulating currents within the single HBDC and among the multiple HBDCs can be suppressed effectively. Furthermore, from Fig. 7 (a), it can be seen that the proposed control method is decentralized, which does not need information of other HBDCs.

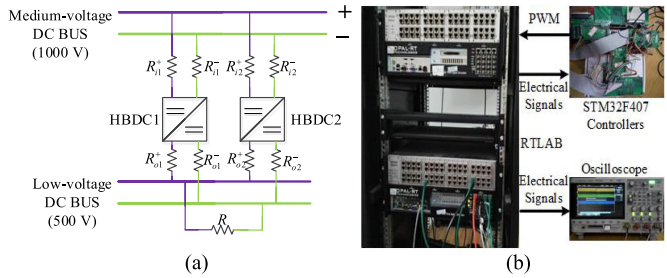

Fig. 8. HIL platform setup. (a) Simulated dc distribution network. (b) Equipment of HIL tests.

TABLE II
CONTROL PARAMETERS OF IPOP HBDCS

Second Degree of Freedom	Value
Droop controller	$v^*_{\rm dc} = 500$ V $r_1 = r_2 = 0.3$ V/A
Voltage controller	$k_{vP} = 1.0$ A/V $k_{vI} = 100.0$ A/Vs
Current controller	$k_{iP} = 0.01$ A^{-1}
First degree of freedom	**Value**
Current controller	$k_{\rm CP} = 0.002$ A^{-1} $k_{\rm CI} = 0.15$ (As)$^{-1}$

Hence, it can save the cost of communication devices and it is easy to implement. Furthermore, it is suitable for modular application very well. On the other hand, though the proposed control method is demonstrated by two IPOP HBDCs, it can be generalized to N $(N > 2)$ IPOP HBDCs.

IV. HARDWARE-IN-LOOP TESTS

To verify the effectiveness of the proposed control method, the corresponding HIL tests are conducted. The studied dc distribution network system is simulated by four parts including the medium-voltage dc bus, the low-voltage dc bus, two IPOP HBDCs, and the resistive dc load as shown in Fig. 8 (a). The HIL platform is based on the RTLAB and STM32F407 MCUs, which is shown in Fig. 8 (b).

The rated medium voltage is 1000 V and the rated low voltage is 500 V. The medium voltage is fixed and the low voltage is obtained through the IPOP HBDCs to convert the voltage levels. Hence, the medium-voltage side is viewed as the input terminal, whereas the low-voltage side is viewed as the output terminal. The dc load is resistive whose resistance is 2 Ω. The topology of the two IPOP HBDCs is the same as Fig. 2 (a), the related electrical parameters are the same as Table I but the output line resistances are changed into $R^+_{o1} = 5$ mΩ, $R^-_{o1} = 10$ mΩ, $R^+_{o2} = 20$ mΩ, $R^-_{o2} = 10$ mΩ. The related control parameters are shown in Table II.

Fig. 9 shows the dynamics of the system when the different degree of freedom control is enabled. Fig. 9 (a) shows control effects of the first degree of freedom control. When there is no any suppression strategy, the output currents are $i^+_{o1} \approx 183$ A, $i^-_{o1} \approx 144$ A, $i^+_{o2} \approx 71$ A, $i^-_{o2} \approx 110$ A. The circulating currents within the single HBDC are obvious and the port degradation is

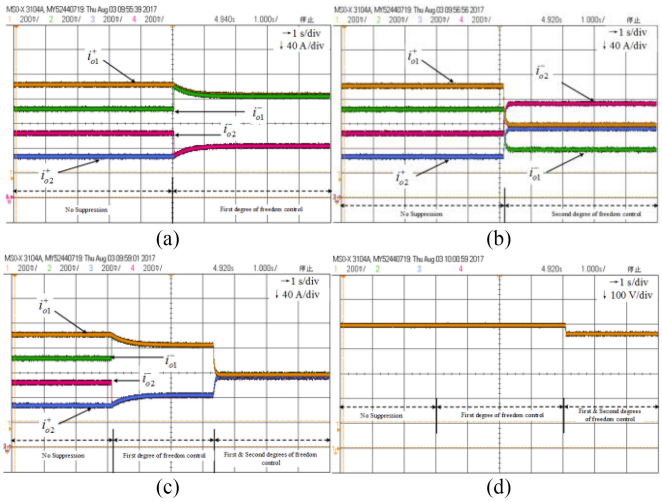

Fig. 9. Dynamics of IPOP HBDCs when different degree of freedom control is enabled. (a) Output currents of IPOP HBDCs when only the first degree of freedom control is enabled. (b) Output currents when only the second degree of freedom control is enabled. (c) Output currents when both the first and the second degrees of freedom control are enabled. (d) Output low voltage when both the first and the second degrees of freedom control are enabled.

serious. From the figure, it can be visually understood that the port degradation will influence the relay protection and some port-based control methods. Furthermore, the output currents of various HBDCs are also different, that is, there exist the circulating currents among the multiple HBDCs. In conclusion, when there is no any suppression strategy, there exist multiple types of circulating currents among IPOP HBDCs. Then, when the first degree of freedom control is enabled, the positive and negative output currents become the same, which are $i^+_{o1} = i^-_{o1} \approx 170$ A, $i^+_{o2} = i^-_{o2} \approx 84$ A. The circulating currents within the single HBDC can be suppressed effectively with the first degree of freedom control. However, the circulating currents among the multiple HBDCs still exist. This result means that the two degrees of freedom control strategies are decoupled and can work independently, which can make the control strategies more flexible. Thus, we can choose the different degree of freedom control according to the actual demands.

Fig. 9 (b) shows the control effects of the second degree of freedom control. Similarly, when there is no any suppression strategy, the output currents are $i^+_{o1} \approx 183$ A, $i^-_{o1} \approx 144$ A, $i^+_{o2} \approx 71$ A, $i^-_{o2} \approx 110$ A. There exist multiple types of circulating currents among IPOP HBDCs. Then, when the second degree of freedom control is enabled, the output currents become $i^+_{o1} = 120$ A, $i^-_{o1} \approx 80$ A, $i^+_{o2} = 116$ A, $i^-_{o2} \approx 156$ A. The second degree of freedom is based on droop control and adopts the positive output currents as feedback signals, hence, the positive output currents i^+_{o1} and i^+_{o2} become approximately equal. But it cannot ensure that the negative output currents i^-_{o1} and i^-_{o2} are equal. Combining Fig. 9 (a) and (b), it can be concluded that only the first degree of freedom control or only the second degree of freedom control cannot eliminate all kinds of circulating currents completely.

Fig. 9 (c) shows the control effects when both the first degree of freedom control and the second degree of freedom

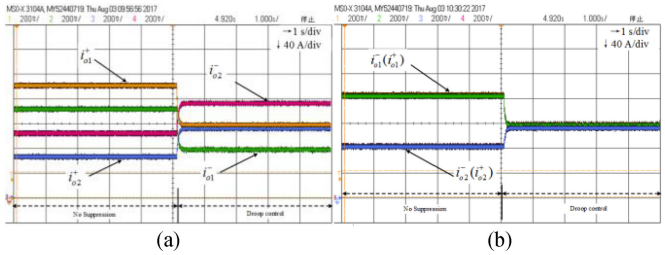

Fig. 10. Effects of droop control applied to (a) IPOP HBDCs and (b) ISOP HBDCs.

control are enabled. As the figure shows, through enabling the control strategies in succession, the control effects of two degrees of freedom control are clearly presented. When both the first degree of freedom control and the second degree of freedom control are enabled, the output currents become $i_{o1}^{+} = i_{o1}^{-} \approx i_{o2}^{+} = i_{o2}^{-} \approx 120$ A. That is, both the circulating currents within the single HBDC and the circulating currents among the multiple HBDCs are suppressed effectively by the proposed two degrees of freedom control method.

Fig. 9 (d) shows the voltage of the low-voltage dc bus. From the figure, it can be seen that the output voltage of the IPOP HBDCs can be maintained within reasonable range (465–500 V) under the control of the proposed two degrees of freedom control method. Because of the droop control, when the second degree of freedom control is enabled, there are some voltage sags. Furthermore, it can be concluded that the first degree of freedom control has few effects on the output voltage of IPOP HBDCs.

Fig. 10 shows the control effects of droop control when it is applied into IPOP HBDCs and ISOP HBDCs. The topology of the tested ISOP HBDCs is presented in Fig. 2 (b). The parameters of two kinds of HBDCs are the same. Fig. 10 (a) shows the control effects of droop control in IPOP HBDCs, which is the same as Fig. 9 (b). As the figure shows, before the droop control is enabled $i_{o1}^{+} \approx 183$ A, $i_{o1}^{-} \approx 144$ A, $i_{o2}^{+} \approx 71$ A, $i_{o2}^{-} \approx 110$ A. After the droop control is enabled $i_{o1}^{+} = 120$ A, $i_{o1}^{-} \approx 80$ A, $i_{o2}^{+} = 116$ A, $i_{o2}^{-} \approx 156$ A. The two positive output currents of IPOP HBDCs became approximately equal, but the negative output currents are still unequal. Therefore, the conventional droop control cannot completely suppress the circulating currents among IPOP HBDCs.

Fig. 10 (b) shows the control effects of droop control in ISOP HBDCs. As the figure shows, before the droop control is enabled $i_{o1}^{+} = i_{o1}^{-} \approx 160$ A, $i_{o2}^{+} = i_{o2}^{-} \approx 80$ A. This results means that the asymmetry of output line resistances does not cause circulating currents within the single HBDC and port degradation, which is very different from the IPOP HBDCs. After the droop control is enabled $i_{o1}^{+} = i_{o1}^{-} = 120$ A, $i_{o2}^{+} = i_{o2}^{-} = 120$ A. That is, the output currents of ISOP HBDCs become equal and circulating currents are suppressed effectively. Through comparison, it can be concluded that the types of circulating currents among IPOP HBDCs are increased compared to the ISOP HBDCs. And the suppression of circulating currents among IPOP HBDCs is more difficult and challenging.

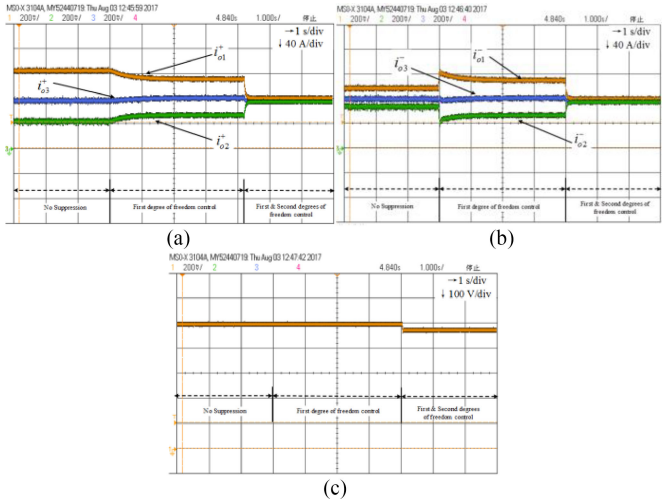

Fig. 11. Control effects when the proposed control method is applied to three IPOP HBDCs. (a) Positive output currents. (b) Negative output currents. (c) Output low voltage.

The related theoretical analyses and the derivation of the proposed control methods are based on two IPOP HBDCs, but the proposed control methods can be applied to the dc distribution networks containing N $(N > 2)$ IPOP HBDCs. Fig. 11 shows the control effects of the proposed two degrees of freedom control when the system contains three IPOP HBDCs, where the output line resistances of the HBDC3 are $R_{o3}^{+} = 10$ mΩ, $R_{o3}^{-} = 10$ mΩ, the other electrical parameters and control parameters are the same as those of the HBDC1 and HBDC2.

Fig. 11 (a) and (b) show the positive and negative output currents of the three IPOP HBDCs under the proposed two degrees of freedom control method, respectively. When there is no any suppression strategy, the output currents are $i_{o1}^{+} \approx 124$ A, $i_{o1}^{-} \approx 96$ A, $i_{o2}^{+} \approx 44$ A, $i_{o2}^{-} \approx 72$ A, $i_{o3}^{+} \approx 80$ A, $i_{o3}^{-} \approx 80$ A. There exist multiple types circulating currents among IPOP HBDCs. Then, when the first degree of freedom control is enabled, the output currents become $i_{o1}^{+} = i_{o1}^{-} \approx 112$ A, $i_{o2}^{+} = i_{o2}^{-} \approx 56$ A, $i_{o3}^{+} = i_{o3}^{-} \approx 80$ A. That is, the circulating currents within the single HBDCs are eliminated effectively through first degree of freedom control. At last, when the second degree of freedom control is enabled, the output currents become $i_{o1}^{+} = i_{o1}^{-} \approx 80$ A, $i_{o2}^{+} = i_{o2}^{-} \approx 80$ A, $i_{o3}^{+} = i_{o3}^{-} \approx 80$ A. That is, the circulating currents among the multiple HBDCs are eliminated effectively through the second degree of freedom control. Combing the above two points, the proposed control method can suppress all kinds of circulating currents among IPOP HBDCs completely. Fig. 11 (c) shows the voltage of the low-voltage dc bus. From the figure, it can be seen that the output voltage of the IPOP HBDCs can be maintained within reasonable range under the control of the proposed control method.

In conclusion, the proposed decentralized two degrees of freedom control method can be well applied to the dc distribution networks containing N (N>2) IPOP HBDCs. The whole control method is not influenced by the number of HBDC modules. Hence, the proposed control method is suitable for module application very well.

V. Conclusion

In this paper, a decentralized two degrees of freedom control method is proposed to suppress the circulating currents among IPOP HBDCs in dc distribution networks. First, the detailed mathematic models of circulating currents among IPOP HBDCs are derived. Through the model, the complicated characteristics of the circulating currents are studied. It is found that there are multiple types of circulating currents in the system, including circulating currents within the single HBDC and the circulating currents among the multiple HBDCs. Hence, the suppression of circulating currents among IPOP HBDCs is a multiobjective control problem. In the paper, it is proven that the conventional one degree of freedom control based on the bipolar modulation cannot eliminate all the circulating currents. Second, based on the model and analysis of circulating currents among IPOP HBDCs, a novel two degrees of freedom control method is proposed to suppress all kinds of circulating currents based on the improved modulation way of HBDCs, which consists of two parts. The droop-based control namely the second degree of freedom control is used to suppress the circulating currents among the multiple HBDCs, while the common mode control namely the first degree of freedom control is used to control the circulating currents within the single HBDC. At last, the real-time hardware-in-loop tests are conducted to verify the effectiveness of the proposed control method.

References

[1] Y. Xia, W. Wei, Y. Peng, P. Yang, and M. Yu, "Decentralized coordination control for parallel bidirectional power converters in a grid-connected DC microgrid," *IEEE Trans. Smart Grid*, to be published, doi: 10.1109/TSG.2017.2725987.

[2] S. Anand and B. G. Fernandes, "Reduced-order model and stability analysis of low-voltage DC microgrid," *IEEE Trans. Ind. Electron.*, vol. 60, no. 11, pp. 5040–5049, Nov. 2013.

[3] H. Mohsenian-Rad and A. Davoudi, "Towards building an optimal demand response framework for DC distribution networks," *IEEE Trans. Smart Grid*, vol. 5, no. 5, pp. 2626–2634, Sep. 2014.

[4] Y. Tan, Y. Li, Y. Cao, and M. Shahidehpour, "Integrated optimization of network topology and DG output for MVDC distribution systems," *IEEE Trans. Power Syst.*, to be published, doi: 10.1109/TPWRS.2017.2688127.

[5] Y. Gu, W. Li, and X. He, "Analysis and control of bipolar LVDC grid with DC symmetrical component method," *IEEE Trans. Power Syst.*, vol. 31, no. 1, pp. 685–694, Jan. 2016.

[6] L. Asiminoaei, E. Aeloiza, P. N. Enjeti, and F. Blaabjerg, "Shunt active-power-filter topology based on parallel interleaved inverters," *IEEE Trans. Ind. Electron.*, vol. 55, no. 3, pp. 1175–1189, Mar. 2008.

[7] B. Wei, J. M. Guerrero, X. Guo, and J. C. Vasquez, "A circulating-current suppression method for parallel connected voltage source inverters (VSI) with common DC and AC buses," *IEEE Trans. Ind. Appl.*, vol. 53, no. 4, pp. 3758–3769, Jul./Aug. 2017, doi: 10.1109/TIA.2017.2681620.

[8] J. Shi, L. Zhou, and X. He, "Common-duty-ratio control of input-parallel output-parallel (IPOP) connected DC–DC converter modules with automatic sharing of currents," *IEEE Trans. Power Electron.*, vol. 27, no. 7, pp. 3277–3291, Jul. 2012.

[9] J. Shi, T. Liu, J. Cheng, and X. He, "Automatic current sharing of an input-parallel output-parallel (IPOP)-connected DC–DC converter system with chain-connected rectifiers," *IEEE Trans. Power Electron.*, vol. 30, no. 6, pp. 2997–3016, Jun. 2015.

[10] D. Liu, F. Deng, Z. Gong, and Z. Chen, "Input-parallel output-parallel (IPOP) three-level (TL) DC/DC converters with interleaving control strategy for minimizing and balancing capacitor ripple currents," *IEEE J. Emerg. Sel. Topics Power Electron.*, vol. 5, no. 3, pp. 1122–1132, Sep. 2017, doi: 10.1109/JESTPE.2017.2649221.

[11] C. Liu *et al.*, "Magnetic-coupling current-balancing cells based input-parallel output-parallel LLC resonant converter modules for high-frequency isolation of DC distribution systems," *IEEE Trans. Power Electron.*, vol. 31, no. 10, pp. 6968–6979, Oct. 2016.

[12] J. Gordillo and C. Aguilar, "A simple sensorless current sharing technique for multiphase DC–DC buck converters," *IEEE Trans. Power Electron.*, vol. 32, no. 5, pp. 3480–3489, May 2017.

[13] H. Mao, L. Yao, C. Wang, and I. Batarseh, "Analysis of inductor current sharing in nonisolated and isolated multiphase dc–dc converters," *IEEE Trans. Ind. Electron.*, vol. 54, no. 6, pp. 3379–3388, Dec. 2007.

[14] A. C. Schittler, D. Pappis, C. Rech, A. Campos, and M. A. D. Costa, "Generalized state-space model for the interleaved buck converter," in *Proc. 9th Brazilian Power Electron. Conf.*, 2011, pp. 451–457.

[15] Y. H. Liao, H. C. Chen, H. C. Cheng, Y. L. Ke, and Y. T. Li, "A novel control strategy of circulating currents in paralleled single-phase boost converters with different power sharing for microgrid applications," *IEEE Trans. Ind. Appl.*, vol. 50, no. 2, pp. 1304–1312, Mar. 2014.

[16] Y. H. Liao and H. C. Chen, "Simplified PWM with switching constraint method to prevent circulating currents for paralleled bidirectional AC/DC converters in grid-tied system using graphic analysis," *IEEE Trans. Ind. Electron.*, vol. 62, no. 7, pp. 4573–4586, Jul. 2015.

[17] P. H. Huang, P. C. Liu, W. Xiao, and M. S. El Moursi, "A novel droop-based average voltage sharing control strategy for DC microgrids," *IEEE Trans. Smart Grid*, vol. 6, no. 3, pp. 1096–1106, May 2015.

[18] X. Lu, J. M. Guerrero, K. Sun, and J. C. Vasquez, "An improved droop control method for DC microgrids based on low bandwidth communication with DC bus voltage restoration and enhanced current sharing accuracy," *IEEE Trans. Power Electron.*, vol. 29, no. 4, pp. 1800–1812, Apr. 2014.

[19] Y. Xia, Y. Peng, H. Hu, Y. Wang, and W. Wei, "Advanced unified decentralised control method with voltage restoration for DC microgrids," *IET Renewable Power Gener.*, vol. 10, no. 6, pp. 861–871, Jun. 2016.

[20] R. Zhu, M. Liserre, Z. Chen, and X. Wu, "Zero-sequence voltage modulation strategy for multiparallel converters circulating current suppression," *IEEE Trans. Ind. Electron.*, vol. 64, no. 3, pp. 1841–1852, Mar. 2017.

[21] C. T. Pan and Y. H. Liao, "Modeling and coordinate control of circulating currents in parallel three-phase boost rectifiers," *IEEE Trans. Ind. Electron.*, vol. 54, no. 2, pp. 825–838, Apr. 2007.

[22] X. Zhang, J. Chen, Y. Ma, Y. Wang, and D. Xu, "Bandwidth expansion method for circulating current control in parallel three-phase PWM converter connection system," *IEEE Trans. Power Electron.*, vol. 29, no. 12, pp. 6847–6856, Dec. 2014.

[23] X. Zhang, T. Wang, X. Wang, G. Wang, Z. Chen, and D. Xu, "A coordinate control strategy for circulating current suppression in multiparalleled three-phase inverters," *IEEE Trans. Ind. Electron.*, vol. 64, no. 1, pp. 838–847, Jan. 2017.

[24] X. Wang *et al.*, "Decentralized impedance specifications for small-signal stability of DC distributed power systems," *IEEE J. Emerg. Sel. Topics Power Electron.*, vol. 5, no. 4, pp. 1578–1588, Dec. 2017.

[25] X. Zhang, X. Ruan, and C. K. Tse, "Impedance-based local stability criterion for DC distributed power systems," *IEEE Trans. Circuits Syst. I, Reg. Paper*, vol. 62, no. 3, pp. 916–925, Jan. 2015.

[26] F. Ji, J. Xiang, W. Li, and Q. Yue, "A feedback passivation design for DC microgrid and its DC/DC converters," *Energies*, vol. 10, no. 1, pp. 14–29, Dec. 2016.

[27] Y. Gu, W. Li, and X. He, "Passivity-based control of DC microgrid for self-disciplined stabilization," *IEEE Trans. Power Electron.*, vol. 30, no. 5, pp. 2623–2632, Sep. 2015.

Yanghong Xia (S'16) was born in Hubei Province, China, in 1991. He received the B.S. degree in automation from the College of Automation, Huazhong University of Science and Technology, Wuhan, China, in 2014. He is currently working toward the Ph.D. degree at the College of Electrical Engineering, Zhejiang University, Hangzhou, China.

His current research interests include nonlinear control, distributed generations, and microgrids.

Yue Li (S'17) received the B.S. degree in electrical engineering from the College of Automation, Wuhan University of Technology, Wuhan, China, in 2017. She is currently working toward the Ph.D. degree at the College of Electrical Engineering, Zhejiang University, Hangzhou, China.

Her current research interests include modeling and control of hybrid microgrids and complex behavior of distributed generations.

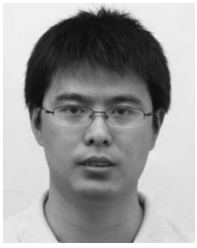

Yonggang Peng (M'16) received the B.S. degree in automation, M.S and Ph.D degrees in control theory and control engineering from the College of Electrical Engineering, Zhejiang University, Hangzhou, China, in 2001, 2004 and 2008, respectively.

He is currently a Professor with the College of Electrical Engineering, Zhejiang University. His research interests include distributed generations, microgrids, and intelligent control.

Miao Yu (M'16) received the B.S. degree in automation and the Ph.D. degree in control science and engineering from the College of Electrical Engineering, Zhejiang University, Zhejiang, China, in 2007 and 2012.

From 2013 to 2015, he was working with Aalto University, Espoo, Finland as a Postdoctoral Researcher. Since 2016, he has been working with the College of Electrical Engineering, Zhejiang University, Zhejiang, China, as a Lecturer. He has authored or co-authored more than 20 technical papers in journals and conferences. His current research interests include control strategies in microgrids and renewable power generation.

Wei Wei received the B.S. degree in automation, M.S degree in control theory and control engineering, and Ph.D degrees in power electronics and electronic drives from the College of Electrical Engineering, Zhejiang University, Hangzhou, China, in 1983, 1986, and 1994, respectively.

Since 1986, he has been with the College of Electrical Engineering, Zhejiang University, Zhejiang, China, where he is currently a Professor. His current research interests include intelligent control, the development of novel technology in renewable energy, and smart grids.